

Model Atmosphere Analysis of the Weakly Magnetic DZ White Dwarf G165-7

P. Dufour¹ P. Bergeron¹, G. D. Schmidt² James Liebert², H. C. Harris³, G.R. Knapp⁴, S.F. Anderson⁵, and D.P. Schneider⁶

ABSTRACT

A reanalysis of the strongly metal-blanketed DZ white dwarf G165-7 is presented. An improved grid of model atmospheres and synthetic spectra is used to analyze *BVRI*, *JHK*, and *ugriz* photometric observations as well as a high quality Sloan Digital Sky Survey spectrum covering the energy distribution from 3600 to 9000 Å. The detection of splitting in several lines of Ca, Na, and Fe, suggesting a magnetic field of $B_s \sim 650$ kG, is confirmed by spectropolarimetric observations that reveal as much as $\pm 7.5\%$ circular polarization in many of the absorption lines, most notably Na, Mg, and Fe. Our combined photometric and spectroscopic fit yields $T_{\text{eff}} = 6440$ K, $\log g = 7.99$, $\log (\text{H}/\text{He}) = -3.0$ and $\log (\text{Ca}/\text{He}) = -8.1$. The other heavy elements have solar ratios with respect to calcium, with the exception of Na and Cr that had to be reduced by a factor of two and three, respectively. A crude polarization model based upon the observed local spectral flux gradient yields a longitudinal field of 165 kG, consistent with the mean surface field inferred from the Zeeman splitting. The inclusion of this weak magnetic field in our synthetic spectrum calculations, even in an approximate fashion, is shown to improve our fit significantly.

Subject headings: stars: abundances – stars: atmospheres – stars: magnetic field – white dwarfs – stars: individual (G165-7)

¹Département de Physique, Université de Montréal, C.P. 6128, Succ. Centre-Ville, Montréal, Québec, Canada H3C 3J7; dufourpa@astro.umontreal.ca, bergeron@astro.umontreal.ca

²Steward Observatory, University of Arizona, 933 North Cherry Avenue, Tucson, AZ 85721; gschmidt@as.arizona.edu, liebert@as.arizona.edu

³US Naval Observatory, P.O. Box 1149, Flagstaff, AZ 86002-1149; hch@nofs.navy.mil

⁴Princeton Univ. Obs., Peyton Hall, Princeton, NJ 08544; gk@astro.princeton.edu

⁵Department of Astronomy, University of Washington, Box 351580, Seattle, WA 98195; anderson@astro.washington.edu

⁶Department of Astronomy and Astrophysics, Pennsylvania State University, 525 Davey Laboratory, University Park, PA 16802; dps@astro.psu.edu

1. INTRODUCTION

White dwarf stars of the DZ spectral type are cool, helium-atmosphere objects showing traces of heavy elements in their optical spectra. They are recognized mainly by the Ca II H & K doublet, while a few also show Ca I $\lambda 4226$, Mg I $\lambda 3835$ or Fe I $\lambda 3730$ (see Sion et al. 1990, Wesemael et al. 1993, and Harris et al. 2003 for typical spectra). Since the heavy elements present in the atmospheric regions sink below the photosphere in a time scale much shorter than the white dwarf cooling time (Paquette et al. 1986), the presence of these metals in DZ stars must be supplied by an external source, the most obvious mechanism being accretion from the interstellar medium, or, in some instances, from a circumstellar dust disk surrounding the white dwarf (Zuckerman & Becklin 1987; Kilic et al. 2005; Becklin et al. 2005). Accretion of comets has also been proposed as a possible origin of metals in the atmospheres of DZ stars (Alcock et al. 1986). A precise determination of the heavy element abundances observed in the optical or UV spectra of DZ stars can thus provide important clues about the accretion rate and chemical composition of the interstellar or circumstellar medium.

Atmospheric abundance analyses of DZ stars are usually based on a restricted number of absorption lines detected in the optical portion of the spectrum (see, e.g. Liebert et al. 1987), although a more important set of lines can be used when UV spectroscopy is available (Zeidler-K.T. et al. 1986; Koester & Wolff 2000; Wolff et al. 2002). G165-7 (WD 1328+307, LHS 2745, $V = 16.03$) is a particularly unusual DZ white dwarf that has practically no flux in the ultraviolet because of the severe blanketing by a large number of metallic lines, but it is also characterized by a very rich optical spectrum showing hundreds of absorption lines from various heavy elements such as Ca, Cr, Fe, Mg and Na. The first model atmosphere analysis of this star was carried out by Wehrse & Liebert (1980) who found $T_{\text{eff}} = 7500 \pm 300$ K, $\log g = 8.0 \pm 0.3$, $\log (\text{H}/\text{He}) < -4.0$, and abundances for the heavy elements of about 1/30 of the solar value under the assumption of scaled solar abundances. Their analysis was based on low and moderate (3–5 Å) resolution spectroscopy in several segments covering the 3350–6700 Å region, as well as on the multichannel spectrophotometry of Greenstein (1976).

Bergeron, Leggett, & Ruiz (2001, hereafter BLR) also analyzed the broad-band energy distribution (optical *BVRI* & near-infrared *JHK* photometry) with a grid of pure helium model atmospheres and found $T_{\text{eff}} = 7320$ K and $\log g = 8.21$ (the surface gravity in this case is constrained by the trigonometric parallax). However, analyses of the energy distribution of DQ white dwarfs based on pure helium models tend to overestimate the effective temperature by 300–800 K and the surface gravity by 0.10–0.24 dex with respect to the atmospheric parameters obtained from models that include carbon. This effect is understood in terms of

an increase of the He^- free-free opacity resulting from the additional free electrons (Provencal et al. 2002; Dufour et al. 2005). A similar effect is thus expected in the case of DZ stars.

We present here a reappraisal of the analysis of G165-7 based on our latest metal blanketed atmospheric models and a new high quality spectrum. The observations are described in § 2 while in § 3 we describe our theoretical framework including our model atmosphere and synthetic spectrum calculations. Our detailed analysis is presented in § 4 and our conclusions follow in § 5.

2. OBSERVATIONS

Our analysis relies on both spectroscopic and photometric observations from various sources. The optical spectrum secured by BLR (details of the observations are also provided there) covers the 3500–8300 Å region at a resolution of 6 Å FWHM. A new spectrum has been obtained by the Sloan Digital Sky Survey (SDSS), where the star is detected as SDSS J133059.26+302953.2. The SDSS (York et al. 2000; Stoughton et al. 2002) obtains five-band imaging (Gunn et al. 1998; Lupton et al. 2001; Pier et al. 2003; Gunn et al. 2006) from which objects are selected for spectroscopic observations. The SDSS quasar survey targets point sources with non-stellar colors (Richards et al. 2002), some of which, like G165-7, turn out to be peculiar stars. The spectrum was observed on 7 April 2005. It covers a wavelength range of 3800–9200 Å at a resolution of ~ 3 Å FWHM. The comparison of the two spectra shown in Figure 1 reveals that the agreement in terms of *absolute* fluxes is surprisingly good, apart from the red portion of the BLR spectrum, which suffers from an obvious flux calibration problem. Also indicated at the top of the figure are the most prominent detected absorption features. Most interestingly, a closer examination of the SDSS spectrum reveals the presence of splitting in several atomic lines (e.g. Fe I $\lambda\lambda 5269 - 5328$, Na I D and Ca II $\lambda\lambda 8542 - 8662$), suggesting the presence of a weak magnetic field (see below).

BLR also reported Cousins *BVRI* and CIT *JHK* photometry for G165-7. Also available are SDSS photometric observations in the *ugriz* system (Fukugita et al. 1996; Hogg et al. 2001; Smith et al. 2002; Ivezić et al. 2004). The photometric observations that will be used to determine the effective temperature are reported in Table 1 together with the trigonometric parallax measurement from the Yale parallax catalog (van Altena et al. 1994). The latter will be used to constrain the radius, and thus the surface gravity (or the mass) of the white dwarf (see § 4). Infrared 2MASS photometry is also available for G165-7: $J = 15.402$ (0.044), $H = 15.282$ (0.087), and $K_S = 15.413$ (0.135); although these values are consistent with the BLR measurements reported in Table 1, the corresponding 2MASS errors are larger for H and K_S and they will not be considered further.

3. THEORETICAL FRAMEWORK

Our LTE model atmosphere code is similar to that described by Dufour et al. (2005) for the study of DQ white dwarfs. It is based on a modified version of the code described at length by Bergeron et al. (1995), which is appropriate for pure hydrogen and pure helium atmospheric compositions, as well as mixed hydrogen and helium compositions, while energy transport by convection is treated within the mixing-length theory. One important modification is that metals and molecules are now included in our equation-of-state and opacity calculations (see Dufour et al. 2005, for details). As was the case for DQ white dwarfs, He⁻ free-free is found to be the dominant source of opacity in DZ stars. It is thus important to include all possible sources of electrons in the equation-of-state, and we have included here all elements with $Z \leq 26$. The chemical abundances cannot be determined individually, however, since most of these elements are not observed spectroscopically. We thus initially assume that the relative abundances are consistent with solar ratios, a reasonable assumption according to Wehrse & Liebert (1980, see also Wolff et al. 2002 for other DZ stars) and our own preliminary analysis based on a chemical abundance analysis of the observable elements.

Our model grid covers a range of atmospheric parameters from $T_{\text{eff}} = 4500$ to 12000 K in steps of 500 K, and $\log(\text{Ca/He}) = -7.0$ to -12.0 in step of 0.5 dex, while $\log g$ is kept fixed at 8.0, an assumption that will need to be verified a posteriori. This grid contains no hydrogen. The relative abundances of all elements heavier than helium are set with respect to the calcium abundance in solar ratios. Additional models described in § 4 have been calculated with different relative abundances of metals, models including hydrogen, and in particular models taking into account the presence of a weak magnetic field.

In the context of cool DZ stars, in addition to the increased He⁻ free-free continuum opacity, important ultraviolet absorption features may potentially affect the energy distribution, and thus the atmospheric structure, with respect to pure helium models. Thus, over 4000 of the strongest metal lines — ~ 2600 lines from Fe I alone — are included explicitly in both the model and synthetic spectrum calculations. These lines were selected by taking all lines contributing more than one tenth of the He⁻ free-free opacity in the range $\tau_R = 0.1 - 1.0$ from several models at $\log \text{Ca/He} = -7$ and T_{eff} between 5000 K and 12,000 K. We are confident that our line list includes all the important contributors to the atomic opacity since spectra calculated by increasing the number of lines by an order of magnitude did not have any effect on the emerging spectrum. The line absorption coefficient is calculated using a Voigt profile for every line and every depth point. The line broadening is treated within the impact approximation with van der Waals broadening by neutral helium. Central wavelengths of the transitions, gf values, energy levels, and damping constants are

extracted from the GFALL line list of R. L. Kurucz¹. We will show in § 4.3, however, that magnetic broadening is the dominant broadening mechanism in the case of G165-7.

4. DETAILED ANALYSIS

4.1. Atmospheric Parameter Determination

The first step in the analysis of the observational data is to estimate the effective temperature of the star. Our fitting procedure is similar to that used for our analysis of DQ white dwarfs (Dufour et al. 2005). Briefly, we transform the magnitudes at each bandpass into observed average fluxes f_λ^m using the following equation

$$m = -2.5 \log f_\lambda^m + c_m , \quad (1)$$

where the values of the constants c_m are taken from the latest photometric calibration of Holberg & Bergeron (2006) based on the absolute fluxes of Vega observed by the *Hubble Space Telescope* with the *Space Telescope Imaging Spectrograph* (Bohlin & Gilliland 2004). The resulting energy distributions are related to the model fluxes through the relation

$$f_\lambda^m = 4\pi (R/D)^2 H_\lambda^m , \quad (2)$$

where R is the radius of the star, D its distance from Earth, and H_λ^m is the Eddington flux — which depends on T_{eff} , $\log g$ and the chemical abundances, properly averaged over the corresponding filter bandpass. The fitting procedure relies on the nonlinear least-squares method of Levenberg-Marquardt based on a steepest decent method (Press et al. 1992). The value of χ^2 is taken as the sum over all bandpasses of the difference between the two sides of equation (2), properly weighted by the corresponding observational uncertainties.

We begin by fitting the *BVRI* and *JHK* photometry to obtain an initial estimate of the effective temperature (the *ugriz* photometry is not used at this stage). We assume $\log g = 8.0$ throughout. Since the temperature obtained from the energy distribution depends on the assumed chemical composition, we rely on the spectroscopic observations to constrain the metal abundances. We thus assume the T_{eff} value obtained from the energy distribution and determine the chemical composition by fitting the SDSS spectrum with our grid of synthetic spectra, properly convolved with a Gaussian instrumental profile at 3 Å FWHM.

¹see <http://kurucz.harvard.edu/LINELISTS.html>

The fitting procedure relies on the least-squares method of Levenberg-Marquardt. A new estimate of the effective temperature is then obtained by fitting the photometric observations with models interpolated at the metal abundances determined from the spectroscopic fit (all metal abundances are solar with respect to calcium). The procedure is then iterated until the atmospheric parameters have converged to a consistent photometric and spectroscopic solution.

4.2. Adopted Atmospheric Parameters

As discussed below, the difficulties encountered in fitting the blue region of the optical spectrum caused us to discard for the time being the B magnitude from our fitting procedure (for the same reason, we fitted only the 5000–9000 Å region of the SDSS spectrum). The long baseline provided by the optical VRI and near-infrared JHK photometry yields a sufficiently reliable estimate of the effective temperature. The photometric and spectroscopic fitting technique described above yields $T_{\text{eff}} = 6440 \pm 210$ K and $\log(\text{Ca}/\text{He}) = -8.1 \pm 0.15$ (with all heavy elements assumed to be solar with respect to calcium), where the uncertainties are obtained from the covariance matrix of the fit; our photometric fit will be shown later (§ 4.3). The stellar radius is derived from the solid angle in equation (2) combined with the distance D obtained from the trigonometric parallax measurement. The radius is then converted into $\log g$ (or mass) using evolutionary models similar to those described by Fontaine et al. (2001) but with C/O cores, $q(\text{He}) \equiv \log M_{\text{He}}/M_{\star} = 10^{-2}$, and $q(\text{H}) = 10^{-10}$, which are representative of helium-atmosphere white dwarfs. We find a value of $\log g = 7.99 \pm 0.29$, entirely consistent with our initial assumption of $\log g = 8$ for our model grid. This corresponds to a mass of $0.57 \pm 0.17 M_{\odot}$, in agreement with the mean mass of white dwarf stars (Bergeron et al. 1992; Liebert et al. 2005). Our value of the effective temperature is significantly smaller than the value of $T_{\text{eff}} = 7320$ K obtained by BLR under the assumption of pure helium-atmosphere models. This is a direct consequence of the increased He^{-} free-free opacity in our model calculations. Because of their higher temperature estimate, BLR required a smaller solid angle to match the photometric observations, which translated into a smaller radius and thus a higher surface gravity of $\log g = 8.21$ (or $0.71 M_{\odot}$).

In the remainder of this analysis, we adopt the atmospheric parameters determined above. As mentioned in the previous section, the abundances of all heavy elements are assumed to be solar with respect to calcium, even if they are not detected in the spectrum. In order to test the sensitivity of this assumption on our atmospheric parameter determination, we also calculated a model with our adopted parameters, but by setting the abundances of all non-detected elements to zero. The resulting spectrum is almost identical to that obtained

under the assumption of solar composition with respect to calcium. This is perhaps not too surprising since the non-detected elements do not contribute significantly to the electron population (see below). Hence we feel confident that our basic assumption does not affect the atmospheric parameter determination. In what follows, we will also allow some changes in the abundances of elements observed spectroscopically (in particular hydrogen). But at the end, we will again measure the impact of these changes on our atmospheric parameter determination.

Although the assumption of metallic abundances scaled with respect to solar abundances is appropriate for fitting globally the 5000–9000 Å region, individual lines such as the Na λ 5892 resonance doublet, the Cr λ 5208 and the Fe (\sim 5200 – 5500 Å) absorption features are predicted to be stronger than observed, and the abundances of these elements must be reduced by factors of 2, 3, and 3, respectively, to produce an acceptable fit. Our best resulting fit to the SDSS spectrum is shown in Figure 2 and at a higher resolution in Figure 3. The overall spectrum in Figure 2 is generally well reproduced by our model. In particular, the predicted continuum slope in the red part of the spectrum is entirely consistent with our effective temperature determination, which is based on *VRI* and *JHK* photometric observations. This provides an internal consistency check between our temperature determination and the photometric and spectroscopic observations.

A more detailed comparison of our spectroscopic fit reveals various discrepancies, however. Most noteworthy, the predicted flux in the blue region of the spectrum between 3600 and 4600 Å is considerably larger than that observed. This region can be better reproduced either by reducing the effective temperature or by increasing the iron abundance, but in both cases, the region longward of 4500 Å cannot be matched properly, including the slope of the energy distribution as well as the iron absorption lines between 5200 and 5500 Å, which are then predicted to be much stronger than observed. The UV flux deficiency could perhaps be explained by a missing source of opacity that would partially mask the absorption lines in this region. We have explored adding more lines, continuous opacities from heavy elements, the occupation probability formalism of Hummer & Mihalas (1988), as well as the Ly α wing calculations of Koester & Wolff (2000), but none of these mechanisms were able to reduce the UV flux significantly.

Figure 3 also reveals that most lines are predicted to be narrower and deeper than observed. Our model even predicts some sharp Ca I features around 6160 and 6450 Å that are not observed spectroscopically. The Mg I λ 5175 triplet is also not well reproduced. This asymmetric profile has been interpreted by Wehrse & Liebert (1980) as evidence for quasi-static van der Waals broadening; we postpone our discussion of this feature to § 4.5. Moreover, there appears to be some missing line contribution in the region around 4380

and 4400 Å. Even the location of some absorption lines seems out of place. For instance, a careful examination of the region near 4050, 4150 and 4260 Å indicates that the strongest predicted features are not matched exactly. These small line shifts cannot be accounted for by uncertainties in the SDSS wavelength calibration since the BLR and SDSS spectra agree so perfectly (see Fig. 1). The observed discrepancies could not be improved by including additional metallic lines in our calculations; therefore another explanation must be sought.

4.3. The Presence of a Weak Magnetic Field

The SDSS spectrum in Figure 1 suggests the presence of Zeeman splitting, and a direct comparison of the observed spectrum with our non-magnetic synthetic spectrum in Figure 3 clearly reveals line splitting. The most obvious cases are the Fe I $\lambda\lambda$ 5269 – 5328, Na I D, and the Ca II $\lambda\lambda$ 8542 – 8662 absorption lines. The Fe I lines near 5400 Å are also not well reproduced by our model spectrum. The peculiarity of the iron features observed here is striking when compared with the spectrum of NLTT 40607 (Kawka et al. 2004, see their Fig. 4), another rare cool DZ star similar to G165-7 which, however, does not show any evidence of line splitting.

To our knowledge, the only polarimetric test for a magnetic field on G165-7 is the broadband (3100 – 8600 Å) circular polarimetry obtained by Angel et al. (1981) that yielded $V/I = +0.071 \pm 0.075\%$, or an estimated mean longitudinal field strength $B_e = 230 \pm 240$ kG. New polarimetric measurements were therefore obtained on 2005 December 30 UT and 2006 May 3 UT using the Steward Observatory 2.3m telescope and SPOL spectropolarimeter of GDS. The instrument was configured for low spectral resolution ($\Delta\lambda = 17$ Å) but broad coverage (4200 – 8200 Å); calibration and reduction of the 600 s observational sequences were carried out in the usual manner (e.g., Schmidt et al. 1992b). The results for 2005 Dec., shown in Figure 4, conclusively verify the presence of a magnetic field, with sharp undulations in circular polarization at each of the prominent lines, reaching $V/I = \pm 7.5\%$ at the strongest Mg, Na, and Fe features. Shown by the bold line in Figure 4 is a synthetic polarization spectrum computed for $B_e = 165$ kG from a simple model based on the local spectral flux gradient (e.g. Angel et al. 1981). The modeling technique is adequate for the linear Zeeman effect in the wings of lines but fails in the resolved cores, and thus tends to underestimate the peak excursions in polarization. For a centered dipole field configuration with no limb darkening, the ratio of the mean longitudinal to mean surface field strength B_e/B_s ranges between ± 0.25 for the full range of inclination angles to the dipole axis, therefore B_e is a sensitive indicator of orientation. Analysis of the individual spectropolarimetric observations yields values of $B_e = 162, 140, 156$ kG, with an uncertainty of ~ 15 kG for each

measurement. Thus, there is no evidence for rotation over the 30 min period covered by the observations. However, a clear change occurred between the two epochs, as the amplitude of the polarimetric features in 2006 May is reduced by more than a factor two. For comparison with the Angel et al. (1981) measurement, the net circular polarization of the data in Figure 4 is $-0.034 \pm 0.030\%$, i.e., not significantly different from zero.

In general, detailed calculations of synthetic spectra in the presence of a magnetic field require a special numerical and physical treatment that cannot be easily implemented in a non-magnetic model atmosphere code. However, if we assume that the magnetic field does not affect the atmospheric structure significantly, some simple approximations can be used to include its effects on the emergent spectrum only. For a relatively weak field, which is certainly the case here, we can use the approximation of the linear Zeeman effect to estimate the splitting of the atomic lines. In this regime, the wavelength separation (in Å) between the centroids of the σ components is given by the simple formula

$$\Delta\lambda = 9.34 \times 10^{-13} \lambda_c^2 g_{\text{eff}} B_s , \quad (3)$$

where λ_c is the central wavelength of the line and g_{eff} is the effective Landé factor. We estimate the mean surface field strength from an average value of the line splitting measured for Fe I $\lambda\lambda 5269, 5328, 4383$, and Na $\lambda 5892$, and by assuming $g_{\text{eff}} = 1.0$ for all lines. With this very simple approximation, we find a mean surface magnetic field of $B_s \sim 650$ kG, a value consistent with the mean longitudinal field of $B_e = 165$ kG estimated above. Fields of this strength are not unusual among white dwarfs, but G165-7 represents a rare case of a DZ white dwarf that exhibits sharp enough metallic features to make the magnetic field detectable through Zeeman splitting. Only two other DZ stars are known to exhibit such metallic line splitting: LHS 2534 with $B_s = 1.92$ MG (Reid et al. 2001) and SDSS J015748.15+003315.1 at $B_s = 3.7$ MG (Schmidt et al. 2003).

In order to take into account, even approximately, the presence of the magnetic field in our model calculations, we simply assume that all spectral lines are split into three components of equal strengths separated by a value of $\Delta\lambda$ given by equation (3), with each component having one third of the total line strength in the zero-field calculation (see also Schmidt et al. 1992a). We then recalculate a synthetic spectrum at our previously determined atmospheric parameters by using this approximate treatment.

The resulting spectroscopic fit using the same chemical abundances as above indicates that the iron abundance no longer needs to be reduced by a factor of 3, and that a solar abundance of iron relative to calcium now matches the 5200–5500 Å lines quite well, as shown in Figure 5. The improvement over our non-magnetic calculations can be appreciated

by contrasting these results with those shown in Figure 3. One important consequence of the increased iron abundance is that the flux deficiency problem in the blue region of the spectrum (top panels of Figs. 3 and 5) has been dramatically improved, although it is admittedly not perfect yet. The missing line contribution in the 4380–4400 Å region discussed above is also naturally explained. There are still a few residual discrepancies, however, particularly near the 4100 and 4350 Å regions, but given the crude approximation we used here to take into account the presence of the magnetic field, we feel our solution is quite satisfactory.

The other panels also reveal a better match for several metallic lines, in particular Na I D and Ca II $\lambda\lambda 8542 - 8662$. The inclusion of a weak magnetic field also solves the problems of the sharp Ca I absorption features around 6160 and 6450 Å (third panel), since the line splitting has now broadened these features considerably. There is a small discrepancy near 6560 Å that is most naturally explained by a contribution from hydrogen (H α ; see next section).

Finally, we show in Figure 6 our best fit to the $(B)VRI$ and JHK photometric observations using model fluxes that take into account the presence of a 650 kG magnetic field. Also displayed are the $ugriz$ photometric observations converted into average fluxes using the transformation equations provided by Holberg & Bergeron (2006). The complete energy distribution is well reproduced with our model, with the exception of the u band, which may suffer from atmospheric extinction problems (see Holberg & Bergeron 2006).

4.4. Hydrogen Abundance Determination

Wehrse & Liebert (1980) place a limit on the hydrogen abundance of $\log(\text{H}/\text{He}) < -4$ in G165-7 based on the absence ($W < 2$ Å) of an H α absorption feature. This limit is very sensitive to the assumed effective temperature of the star. Our effective temperature determination is ~ 1000 K cooler than that obtained by Wehrse & Liebert (1980, $T_{\text{eff}} = 7500$ K) so the limit on the hydrogen abundance needs to be increased. Furthermore, a close inspection of the SDSS spectrum, together with our spectroscopic fit (Fig. 5), clearly reveals the presence of a very shallow and broad H α absorption feature. This observed width is actually what is expected at these temperatures since van der Waals broadening by neutral helium is the main broadening mechanism in the physical conditions encountered here. Note also that without a good modeling of the calcium lines in the blue wing of H α , this absorption feature could easily be interpreted as noise. The H α feature cannot be detected in the lower signal-to-noise ratio spectrum displayed in Figure 3 of Wehrse & Liebert (1980).

We find that a model spectrum with $\log (\text{H}/\text{He}) = -3$ reproduces almost perfectly the $\text{H}\alpha$ region (see the insert in Fig. 5). Here, the magnetic field for $\text{H}\alpha$ has been included following the procedure outlined in Bergeron et al. (1992), although its effect on the observed profile is found to be negligible since van der Waals broadening by neutral helium completely dominates in this physical regime. Because of the high metallicity content determined for G165–7, the contribution of hydrogen to the electron population is relatively small, except perhaps in the deepest layers where the temperature is high enough to produce substantial ionization. Actually, at the photosphere ($\tau_R \sim 1$), the principal electron donors are Mg (27.6%), Fe (21.5%), Si (17.1%) and H (24.8%), while Ca and Na contribute 2.0% and 1.7%, respectively. Furthermore, the contributions of the H^- opacity and H_2 collision induced opacity are negligible compared to the dominant He^- free-free opacity. In order to estimate how our atmospheric parameter determination would change given (1) the presence of hydrogen, (2) the reduced abundances of Na and Cr, and (3) the presence of the magnetic field, we fitted our best model spectrum shown in Figure 5 with our hydrogen-free, non-magnetic, solar scaled models. The atmospheric parameters we obtain differ by only 100 K in T_{eff} and 0.2 dex in $\log (\text{Ca}/\text{He})$.

Hydrogen, being the lightest element, tends to raise to the upper layers of the photospheric regions of the star, and its abundance should thus always *increase* with time as the white dwarf experiences multiple episodes of accretion from the interstellar medium. Previous studies (e.g., Dupuis et al. 1993; Wolff et al. 2002) have shown, however, that DZ stars have less hydrogen in their atmospheres than what is expected if the accreted material has a solar composition. Consequently, the hydrogen accretion rate must be reduced relative to that of metals in order to account for the relatively low hydrogen abundances (with respect to heavier elements) observed in DZ stars. One model, proposed by Wesemael & Truran (1982) to reduce the accretion of hydrogen, is the so-called propeller mechanism. In this model, protons are prevented from accreting onto the surface of the white dwarf by a rotating magnetic field, while metals, most probably in the form of grains, are unaffected by this mechanism and thus reach the surface. In addition, this model requires a relatively strong UV radiation flux to ionize hydrogen in the immediate surroundings of the star, a requirement that is certainly not met in the case of G165-7. Since the propeller mechanism cannot prevent hydrogen from being accreted onto the surface of G165-7, we expect the metal-to-hydrogen ratio to be much lower than the solar value, $\log (\text{Ca}/\text{H})_{\odot} = -5.6$. However, the value we determined for G165-7, $\log (\text{Ca}/\text{H}) = -5.1$, is slightly larger than the solar value. G165-7 thus represents another case of a DZ star with a unexpectedly low hydrogen abundance.

4.5. Asymmetric MgI Line or MgH Molecular Absorption?

Based on the absence of $H\alpha$ and their relatively high effective temperature estimate, Wehrse & Liebert (1980) rejected the possibility that the asymmetric Mg I $\lambda 5175$ “b” profile could be explained by a MgH molecular absorption band. Instead, they interpreted the observed asymmetry as evidence that the impact theory was not valid anymore for this line. A quasi-static profile was found to give a reasonable agreement to the shape of the blue wing of the Mg I line if the C_6 damping constant was increased by a factor 120. The lower temperature and higher hydrogen abundance determined here allow us to reconsider this interpretation.

In order to explore this alternative interpretation, we have explicitly included the MgH line opacity in our calculations. Although our code takes into account the formation of molecules in the equation-of-state, the molecular opacity for the coolest stars has not been fully implemented yet, with the exception of the C_2 molecular Swan bands required for analysis of DQ stars (Dufour et al. 2005). Our result, shown in Figure 7, indicates that it is indeed possible to match approximately the blue wing at ~ 5100 Å, but only by increasing the MgH abundance by a factor of ~ 20 . We can only offer tentative explanations to explain this inconsistency.

One possibility is that because of a missing ingredient in our model calculations — an important source of opacity or additional electron donors for instance, our effective temperature determination is still overestimated. If G165-7 is actually cooler than suggested by our models, more hydrogen could be present and molecular formation would be favored. For example, at $T_{\text{eff}} = 6250$ K, the above factor is reduced to 10, but the overall energy distribution predicted is not reproduced as well as with our adopted 6440 K solution. Alternatively, the molecular absorption process could be affected by the magnetic field, but detailed calculations are needed to confirm this hypothesis. We cannot rule out the possibility that we are simply dealing with the breakdown of the impact approximation, as initially proposed by Wehrse & Liebert (1980), but until this feature is correctly fitted within a coherent theoretical framework, we must conclude that the nature of the Mg I asymmetric profile remains uncertain. We note that it is unlikely that non-ideal effects in the equation-of-state (Coulomb corrections, finite volume effect, line quenching) are important since the pressure in our model never exceeds 10^{10} dynes cm^{-2} . Based on a modified version of the equation-of-state of Mihalas et al. (1990), Wolff et al. (2002) found only a weak influence in van Maanen 2, another DZ star in which the atmospheric pressure is certainly higher than that in G165-7 since it is cooler and possesses a smaller metal content. We note finally that the sample of DZ stars displayed in Figures 10 and 11 of Harris et al. (2003) show several objects with similar asymmetric profiles, some of them certainly too hot (~ 8000 K) to be

explained by molecular absorption.

5. SUMMARY AND CONCLUSIONS

Our study of G165-7 represents the first detailed model atmosphere analysis of a magnetic DZ white dwarf. High quality spectroscopic observations revealed that several metallic features were split by a surface magnetic field of approximately 650 kG. We achieved a best fit with a model atmosphere and synthetic spectrum at $T_{\text{eff}} = 6440$ K, $\log g = 7.99$, $\log (\text{H}/\text{He}) = -3$, and $\log (\text{Ca}/\text{He}) = -8.1$, with other heavy elements in solar abundances relative to the calcium abundance (except for Na and Cr whose abundances had to be reduced by factors of 2 and 3, respectively). The predicted emergent spectrum provided an excellent match to the whole energy distribution of G165-7, as well as to most spectral features. By using the approximation of the linear Zeeman effect in our synthetic spectrum calculations, we were able to reproduce the splitting observed in several metallic lines. We also found that, contrary to the original analysis of G165-7 by Wehrse & Liebert (1980), hydrogen is present with an abundance of $\log (\text{H}/\text{He}) \sim -3$. With an effective temperature ~ 1000 K cooler than previously found, the molecular formation of MgH can no longer be completely ruled out. We have shown that the so-called “asymmetric Mg I profile” might possibly be explained by a MgH molecular feature instead of a quasi-static profile, although we cannot be entirely certain of this interpretation until a coherent theoretical framework becomes available. Other spectra of DZ stars with strong metallic absorption features have been found in the SDSS (Harris et al. 2003). Analysis of them may lead to more insight into the properties of G165-7 and whether they are repeated in other DZ stars.

We are grateful to A. Gianninas for a careful reading of this manuscript. The authors thank P. Smith for assistance with the spectropolarimetric observations. Research into magnetic stars and stellar systems at Steward Observatory is supported by NSF grant AST 03-06080 to GDS. This work was supported in part by the NSERC Canada and by the FQRNT (Québec). P. Bergeron is a Cottrell Scholar of Research Corporation.

Funding for the SDSS and SDSS-II has been provided by the Alfred P. Sloan Foundation, the Participating Institutions, the National Science Foundation, the U.S. Department of Energy, the National Aeronautics and Space Administration, the Japanese Monbukagakusho, the Max Planck Society, and the Higher Education Funding Council for England.

The SDSS is managed by the Astrophysical Research Consortium for the Participating Institutions. The Participating Institutions are the American Museum of Natural History, Astrophysical Institute Potsdam, University of Basel, Cambridge University, Case Western

Reserve University, University of Chicago, Drexel University, Fermilab, the Institute for Advanced Study, the Japan Participation Group, Johns Hopkins University, the Joint Institute for Nuclear Astrophysics, the Kavli Institute for Particle Astrophysics and Cosmology, the Korean Scientist Group, the Chinese Academy of Sciences (LAMOST), Los Alamos National Laboratory, the Max-Planck-Institute for Astronomy (MPIA), the Max-Planck-Institute for Astrophysics (MPA), New Mexico State University, Ohio State University, University of Pittsburgh, University of Portsmouth, Princeton University, the United States Naval Observatory, and the University of Washington.

REFERENCES

- Alcock, C., Frstrom, C. C., & Siegelman, R. 1986, *ApJ*, 302, 462
- Angel, J. R. P., Borra, E. F., & Landstreet, J. D. 1981, *ApJS*, 45, 457
- Becklin, E. E., Farihi, J., Jura, M., Song, I., Weinberger, A. J., & Zuckerman, B. 2005, *ApJ*, 632, L119
- Bergeron, P., Leggett, S. K., & Ruiz, M. T. 2001, *ApJS*, 133, 413 (BLR)
- Bergeron, P., Ruiz, M. T., & Leggett, S. K. 1992, *ApJ*, 400, 315
- Bergeron, P., Saffer, R. A., & Liebert, J. 1992, *ApJ*, 394, 228
- Bergeron, P., Saumon, D., & Wesemael, F. 1995, *ApJ*, 443, 764
- Bohlin, R. C., & Gilliland, R. L. 2004, *AJ*, 127, 3508
- Dufour, P., Bergeron, P., & Fontaine, G. 2005, *ApJ*, 627, 404
- Dupuis, J., Fontaine, G., & Wesemael, F. 1993, *ApJS*, 87, 345
- Fontaine, G., Brassard, P., & Bergeron, P. 2001, *PASP*, 113, 409
- Greenstein, J. L. 1976, *ApJ*, 207, L120
- Gunn, J. E., et al. 1998, *AJ*, 116, 3040
- Gunn, J. E., et al. 2006, *AJ*, 131, 2332
- Fukugita, M., Ichikawa, T., Gunn, J. E., Doi, M., Shimasaku, K., & Schneider, D. P. 1996, *AJ*, 111, 1748

- Harris, H. C., et al. 2003, *AJ*, 126, 1023
- Hogg, D. W., Finkbeiner, D. P., Schlegel, D.J., & Gunn, J. E., 2001, *AJ*, 122, 2129
- Holberg, J. B., & Bergeron, P. 2006, *AJ*, in press
- Hummer, D. G., & Mihalas, D. 1988, *ApJ*, 331, 794
- Ivezić, Z., et al. 2004, *Astron. Nachr.*, 325, 583
- Kawka, A., Vennes, S., & Thorstensen, J. R. 2004, *AJ*, 127, 1702
- Kilic, M., von Hippel, T., Leggett, S. K., & Winget, D. E. 2005, *ApJ*, 632, L115
- Koester, D., & Wolff, B. 2000, *A&A*, 357, 587
- Liebert, J., Bergeron, P., & Holberg, J. B. 2005, *ApJS*, 156, 47
- Liebert, J., Wehrse, R., & Green, R. F. 1987, *A&A*, 175, 173
- Lupton, R. H., Gunn, J. E., Ivezić, Ž., Knapp, G. R., Kent, S. M., & Yasuda, N. 2001, in *ASP Conf Ser 238, ADASS X*, ed. F.R. Harnden Jr., F.A. Primini, & H.E. Payne (San Francisco: ASP), p. 269
- Mihalas, D., Hummer, D. G., Mihalas, B. W., & Däppen, W. 1990, *ApJ*, 350, 300
- Paquette, C., Pelletier, C., Fontaine, G., & Michaud, G. 1986, *ApJS*, 61, 197
- Pier, J. R., et al. 2003, *AJ*, 125, 1559
- Press, W. H., Teukolsky, S. A., Vetterling, W. T., & Flannery, B. P. 1992, *Numerical Recipes in FORTRAN*, 2nd edition (Cambridge: Cambridge University Press), 644
- Provencal, J. L., Shipman, H. L., Koester, D., Wesemael, F., & Bergeron, P. 2002, *ApJ*, 568, 324
- Reid, I. N., Liebert, J., & Schmidt, G. D. 2001, *ApJ*, 550, L61
- Richards, G. T., et al. 2002, *AJ*, 123, 2945
- Schmidt, G. D., Bergeron, P., Liebert, J., & Saffer, R. A. 1992a, *ApJ*, 394,603
- Schmidt, G.D., Stockman, H.S., & Smith, P.S. 1992b, *ApJ*, 398, L57
- Schmidt, G. D., et al. 2003, *ApJ*, 595, 1101

- Sion, E. M., Kenyon, S. J., & Aannestad, P. A. 1990, *ApJS*, 72, 707
- Smith, J. A., et al. 2002, *AJ*, 123, 2121
- Stoughton, C., et al. 2002, *AJ*, 123, 485
- van Altena, W. F., Lee, J. T., & Hoffleit, E. D. 1994, *The General Catalogue of Trigonometric Parallaxes* (New Haven: Yale University Observatory)
- Wehrse, R., & Liebert, J. 1980, *A&A*, 86, 139
- Wesemael, F., Greenstein, J. L., Liebert, J., Lamontagne, R., Fontaine, G., Bergeron, P., & Glaspey, J. W. 1993, *PASP*, 105, 761
- Wesemael, F., & Truran, J. W. 1982, *ApJ*, 260, 807
- Wolff, B., Koester, D., & Liebert, J. 2002, *A&A*, 385, 995
- York, D. G., et al. 2000, *AJ*, 120, 1579
- Zeidler-K.T., E.-M., Weidemann, V., & Koester, D. 1986, *A&A*, 155, 356
- Zuckerman, B., & Becklin, E. E. 1987, *Nature*, 330, 138

Table 1. Observational data for G165–7^a

<i>B</i>	<i>V</i>	<i>R</i>	<i>I</i>	<i>J</i>	<i>H</i>	<i>K</i>	<i>u</i>	<i>g</i>	<i>r</i>	<i>i</i>	<i>z</i>	π (mas)
16.73	16.03	15.74	15.60	15.50	15.36	15.34	18.27	16.32	15.92	15.93	16.10	33.4
0.05	0.03	0.03	0.03	0.05	0.05	0.05	0.016	0.003	0.003	0.004	0.007	5.3

^aUncertainties are on the second line. Cousins *BVRI* and CIT *JHK* photometry is from BLR, while the *ugriz* photometry comes from SDSS.

Table 2. Atmospheric Parameters for G165–7

Parameter	Value
T_{eff} (K)	6440 (210)
$\log g$	7.99 (0.29)
M/M_{\odot}	0.57 (0.17)
$\log \text{H/He}$	~ -3
$\log \text{Na/He}$	-8.43 (0.15)
$\log \text{Mg/He}$	-6.88 (0.15)
$\log \text{Ca/He}$	-8.10 (0.15)
$\log \text{Cr/He}$	< -9.30
$\log \text{Fe/He}$	-6.96 (0.15)
B_s (kG)	~ 650
B_e (kG)	~ 165

Fig. 1.— Comparison of absolute fluxes from two independent spectroscopic observations of G165-7 in the optical. The thick line is the SDSS spectrum with a resolution of $\sim 3 \text{ \AA}$ FWHM, while the thin line corresponds to the BLR spectrum at a slightly lower resolution of $\sim 6 \text{ \AA}$ FWHM. The latter suffers from flux calibration problems longward of 6500 \AA (also notice the presence of the Earth’s atmospheric A and B absorption bands in the BLR spectrum). The most important features are labeled at the top. The presence of Zeeman splitting is clearly visible in the SDSS spectrum.

Fig. 2.— Our best fit to the SDSS optical spectrum with a non-magnetic model at $T_{\text{eff}} = 6440 \text{ K}$, $\log g = 7.99$, and $\log (\text{Ca}/\text{He}) = -8.1$. All heavy elements are assumed to be solar with respect to the calcium abundance, with the exception of Na, Cr, and Fe whose abundances are reduced by factors of 2, 3, and 3, respectively. The hydrogen abundance is also set to zero.

Fig. 3.— Same as Fig. 2 but at a higher resolution. Note that the BLR spectrum is used here below 3800 \AA .

Fig. 4.— *Top panel:* Observed circular polarization (*thin line*) and model polarization spectrum (*thick line*) for a mean longitudinal field of 165 kG . *Bottom panel:* Corresponding spectrum obtained with a spectral resolution ($\Delta\lambda = 17 \text{ \AA}$) inadequate to show the Zeeman splitting of the line cores.

Fig. 5.— Same as Fig. 3 but by taking into account the presence of a weak magnetic field with a mean surface field strength of $B_s \sim 650 \text{ kG}$ in our model flux calculations. In this model, the iron abundance is solar with respect to calcium. The insert in the third panel from the top shows our prediction of a weak $\text{H}\alpha$ absorption feature when a small abundance of hydrogen with $\log (\text{H}/\text{He}) = -3$ is included.

Fig. 6.— Our best fit to the energy distribution of G165-7 using models including metals as well as a weak magnetic field. The observations are represented by the error bars while the corresponding average model fluxes are shown by the filled circles (*BVRIJHK*, from left to right) and by the open circles (*ugriz*, from left to right; here the uncertainties have been set to 0.04 for clarity). The atmospheric parameters are given in the figure.

Fig. 7.— Comparison of the observed and synthetic spectra in the $5000 - 5300 \text{ \AA}$ region. Here, the MgH molecular opacity has been included in our calculations (*solid line*), although an increase of the MgH abundance by a factor of 20 was required to match the blue wing of Mg I. We also show our calculations without the inclusion of MgH (*dashed line*).

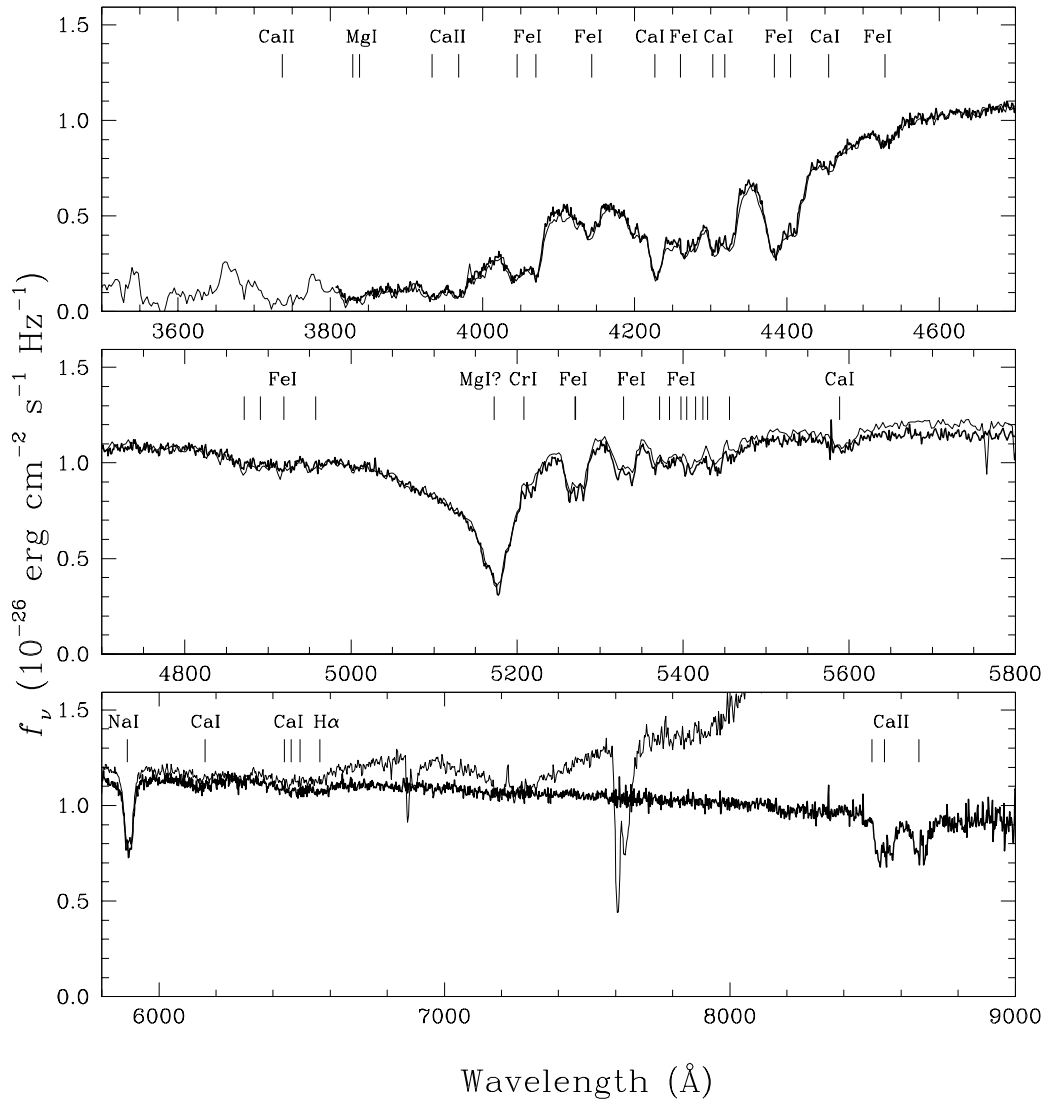


Figure 1

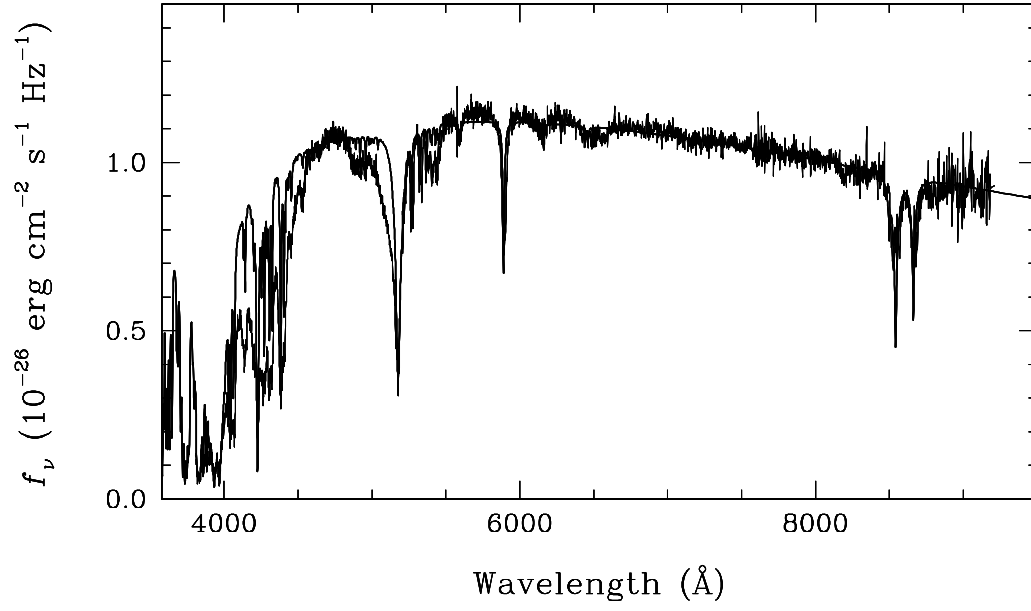


Figure 2

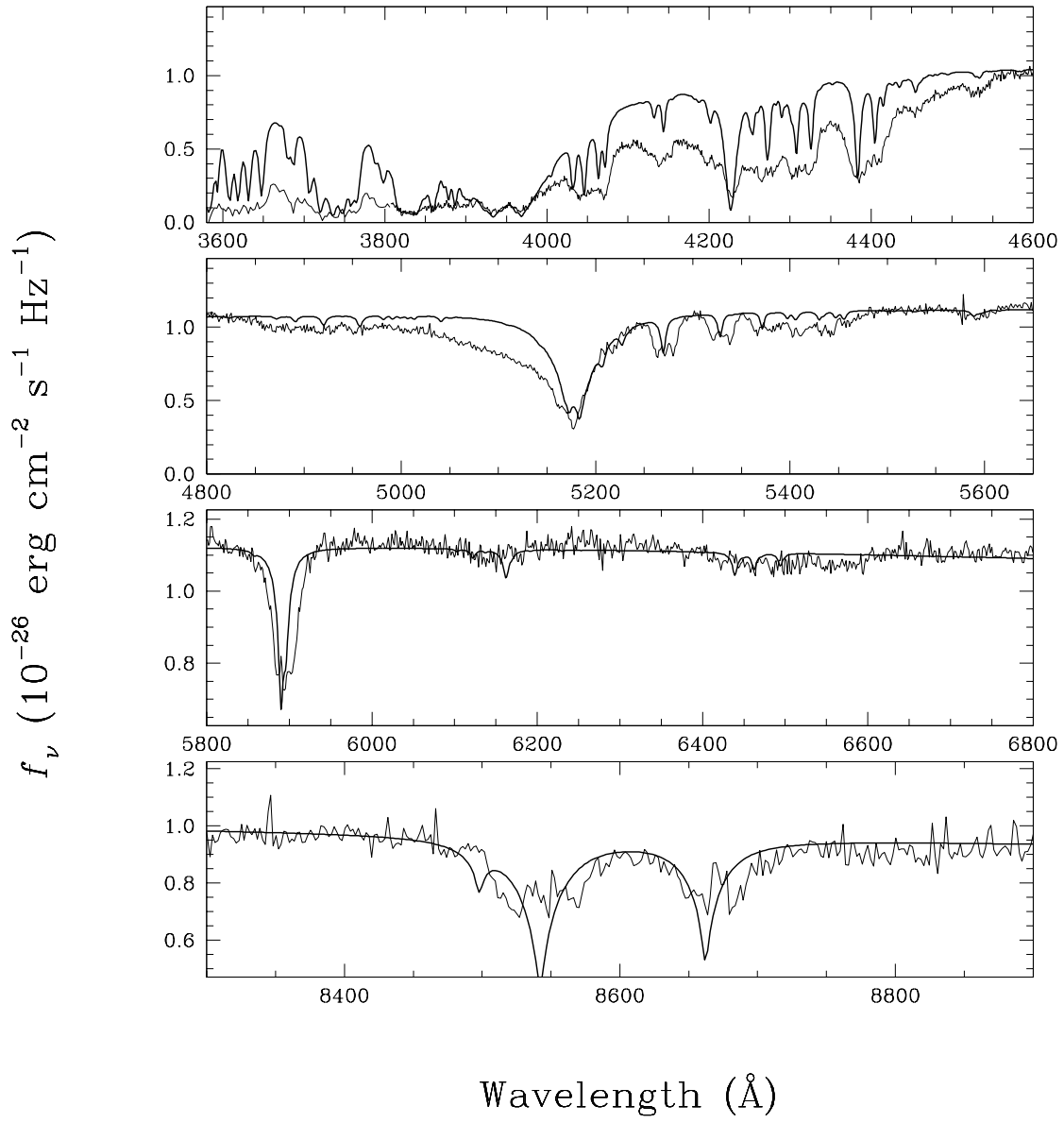


Figure 3

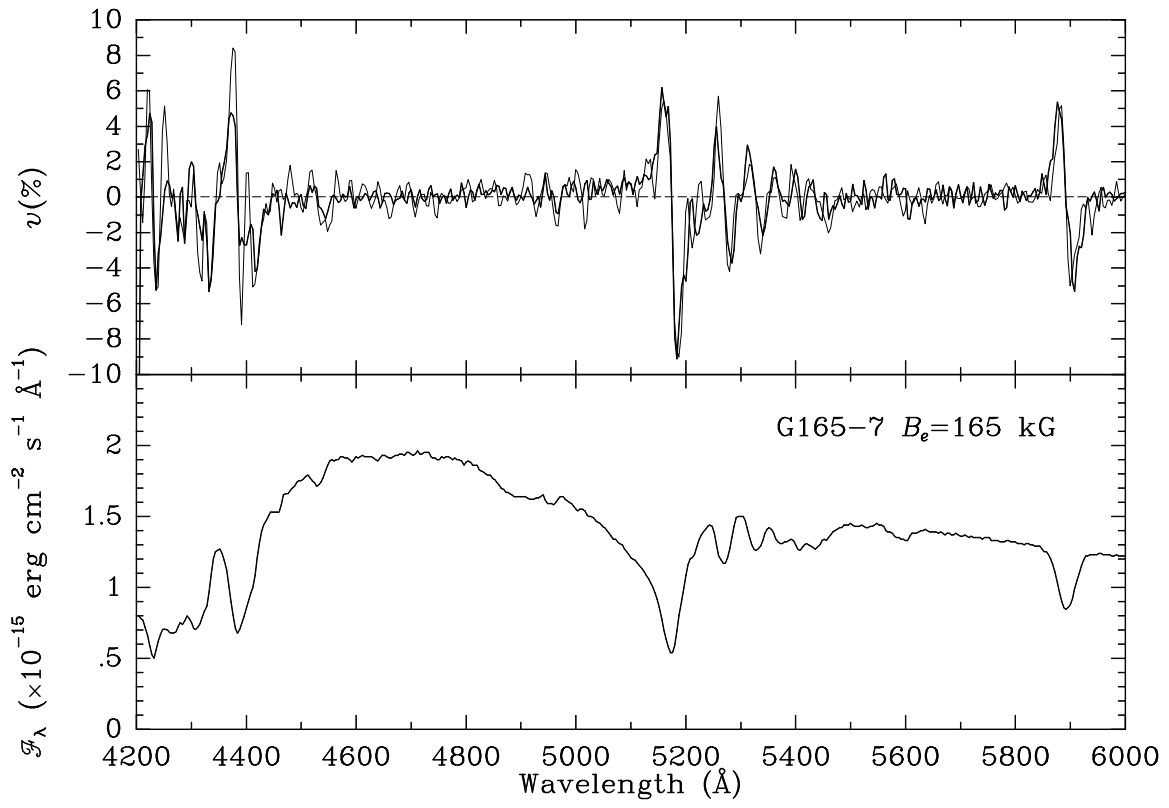


Figure 4

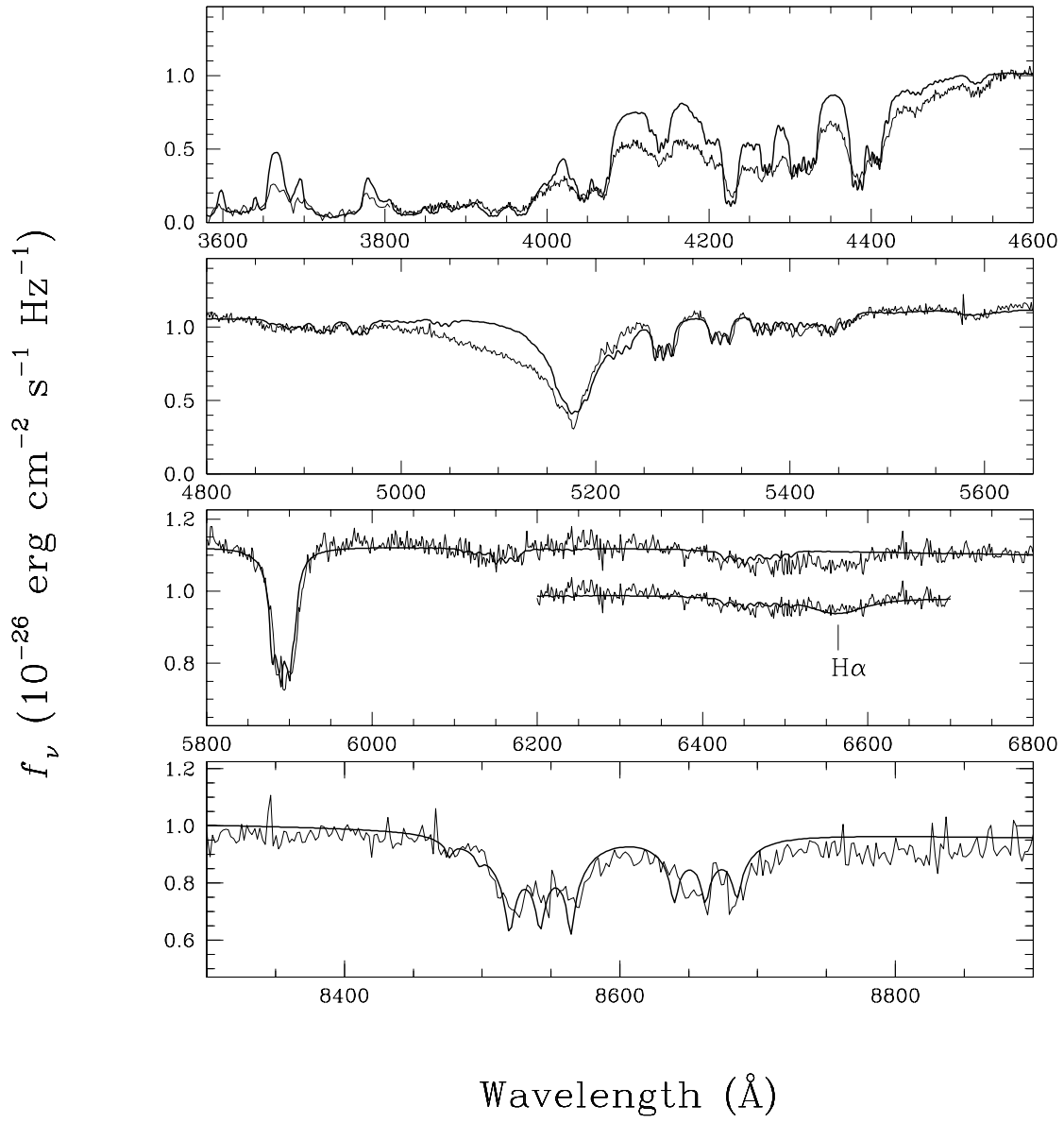


Figure 5

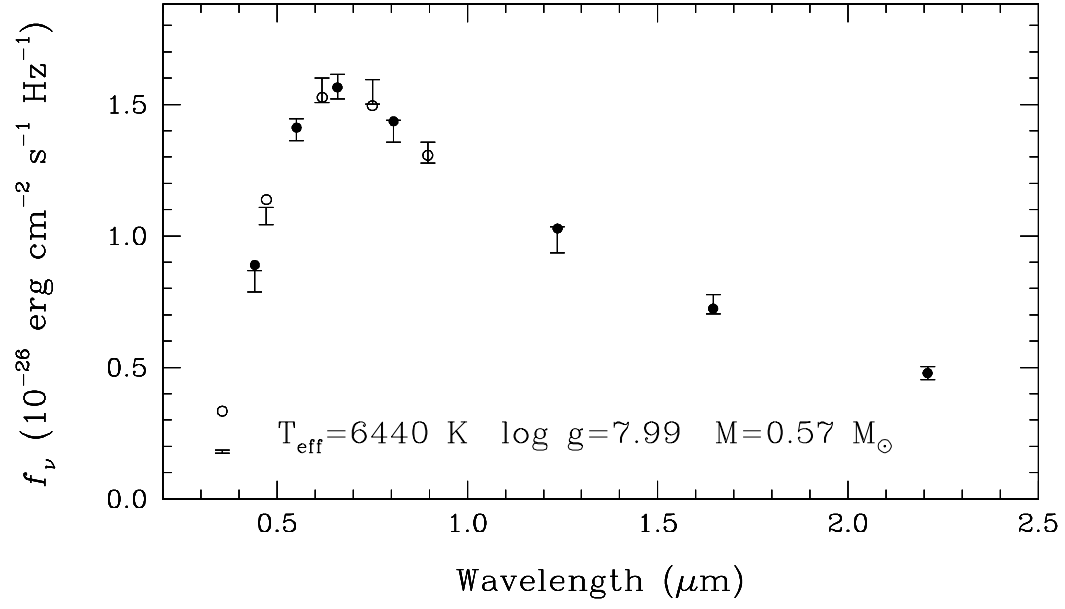


Figure 6

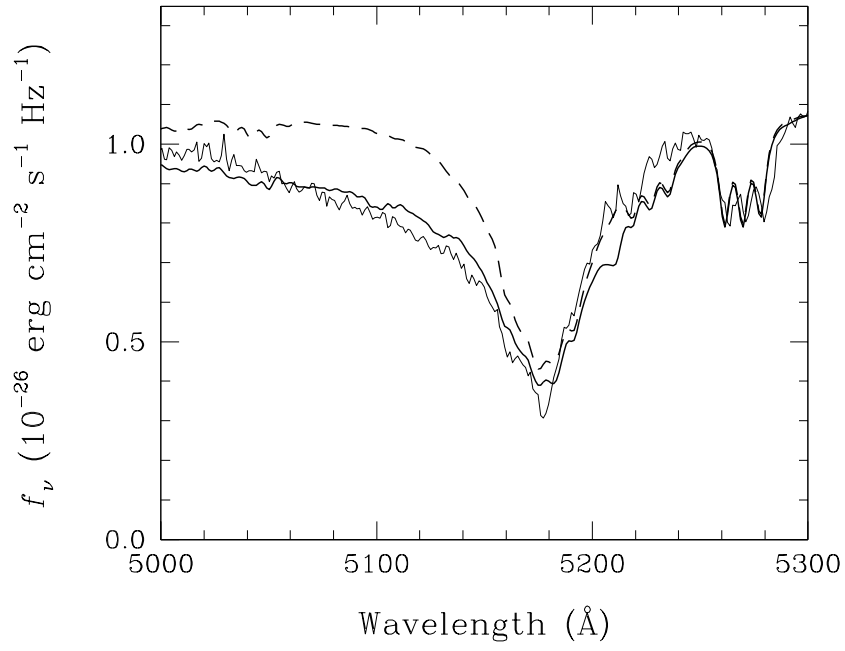


Figure 7